Penerbit Akademia Baru

Journal of Advanced Research in Fluid Mechanics and Thermal Sciences

Journal homepage: www.akademiabaru.com/arfmts.html
ISSN: 2289-7879

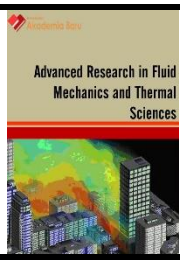

Design and Performance Analysis of a Biomass Fueled Mono-Tube Boiler for Humid Air Turbine Cycle

Open Access

Noor Badshah[1], Khaled Ali Al-Attab[1,*], Zainal Alimuddin Zainal Alauddin[1]

[1] School of Mechanical Engineering, Engineering Campus, Universiti Sains Malaysia, 14300 Nibong Tebal, Penang, Malaysia

ARTICLE INFO

Article history:
Received 13 March 2020
Received in revised form 25 April 2020
Accepted 6 May 2020
Available online 8 June 2020

ABSTRACT

Externally fired gas turbine (EFGT) is one of the few power generation configurations capable of utilizing biomass in its solid form without any additional equipment to convert it to liquid or gas. Due to its high thermal output capability for drying applications, EFGT is one of the most suitable configurations for the off-grid rural areas in Malaysia with abundant biomass waste and high demand of heat for crops drying. The main downside of EFGT is the necessity for high temperature heat exchanger which compromises the system feasibility due to the high cost and other technical challenges. This can be eliminated by the addition of steam in a configuration known as humid air turbine (HAT), thus, limiting the required temperature and allowing for the use of common low-temperature heat exchanger types. Several mono-tube steam boiler designs were compared to fulfil the required steam flow rate of 2 kg/min for the available EFGT system. Counter-flow design was found to be more suitable with its higher efficiency. The boiler was characterized experimentally at output steam flow rate range of 0.4-2 kg/min using off-cut waste wood from furniture industry. Maximum achieved boiler efficiency and specific fuel consumption were 73% and 0.29 kg/kWh, respectively.

Keywords:
Mono-tube boiler; Biomass; Humid Air Turbine; Externally fired gas turbine

1. Introduction

Excessive fossil fuel utilization has led to fuel depletion, global warming and pollution [1]. World Energy Outlook 2007 estimated that the oil and gas supplies will escalate from 36M barrel/day in 2006 to 61M/day in 2030 [2]. According to World Health Organization, the excessive burning of fossil fuels has led to catastrophic health implications with dangerous levels of pollution in major cities in the world [3]. Additionally, the accumulation of greenhouse emissions in the atmosphere from fossil fuel burning resulted in steady elevation in global temperature which is showing an alarming negative impact on weather and environment [4,5]. Thus, the last few decades have witnessed significant increment in renewable fuels research and development for new techniques to utilize them [6].

* *Corresponding author.*
E-mail address: khaled@usm.my (Khaled Ali Al-Attab)

https://doi.org/10.37934/arfmts.72.1.111123

Renewable energy sources such as hydropower, wind, biomass, geothermal and solar are the preferable and most promising fossil fuel alternatives [7]. Biomass fuel is a major candidate as it is readily available per demand unlike most of the other renewable energy sources. Biomass fuel refers to any organic substance from plant materials or animal wastes used as fuels. Biomass includes for example, food crops, grassy and woody plants, agricultural or forestry residues and urban wastes. Biomass fuel combustion does not increase the net carbon dioxide emissions in the atmosphere through the biomass growth cycle where carbon dioxide is removed through photosynthesis process [8]. Small scale distributed co-generation biomass fuelled system has proven its economic viability and was found to be superior in terms of electricity cost and heat supply compared to fossil fuelled systems especially near the biomass fuel sources [9,10]. However, several challenges face the direct utilization of solid biomass as either a total replacement or co-firing with fossil fuels in the existing boilers. Solid biomass suffers from its lower energy density and high moisture which require intensive fuel pre-treatment [11]. This makes the utilization of biomass in its solid form only feasible if the plant is located near the biomass sources. Moreover, thermal engines, other than boilers, which are the internal combustion reciprocating engines and gas turbines are not capable of utilizing biomass in its solid form which require additional biomass conversion process into liquid or gaseous forms.

Biomass is an important type of renewable energy fuel source in Malaysia as it provides more reliable electrical and thermal power source throughout the year with wider distribution compared to solar and wind energy sources [12]. In the Malaysian rural areas, crops drying and biomass waste management are some of the challenges facing the farmers on daily basis. Open crop drying under the sun is not a reliable method with high space requirement [13], especially in Malaysia with its high rainfall rates. Open burning of biomass waste is another environmental issue that raises a big concern in the South-East Asian countries. The use of externally fired gas turbine (EFGT) technology has the potential to solve these issues with high flexibility in the use of low-grade solid fuels and a readily high thermal power output in the form of hot air exiting the turbine [14]. EFGT was widely investigated using theoretical simulation with noticeable lack in experimental investigations due to the high cost and challenges associated with the required high temperature heat exchanger to generate hot air [15,16].

A turbocharger-based EFGT system was developed by Al-Attab and Zainal [17] in previous studies with novel gasifier-combustor design for the direct utilization of wood blocks waste from furniture industry without any pre-treatment. Air is heated in high temperature heat exchanger for the external firing of the turbine and part of the hot air was recuperated back to the gasifier-combustor eliminating the need for any additional air blowers while the rest of the hot air was utilized as thermal power output for crops drying. The turbine inlet temperature (TIT) was limited to about 700°C resulting in inadequate power for the turbine to sustain in the self-operating mode. This is partially attributed to the lower quality and calorific value of biomass fuel that limits the combustion temperature compared to fossil fuel [18]. Although, increasing the heat exchanger surface area can further increase TIT, material stress resistance at elevated temperatures for metal-alloys is commonly limited to 900°C [19]. Evaporative EFGT or humid air turbine (HAT) technology is one of the proposed solutions to increase turbine power without the need for an excessive elevation in TIT [19]. Steam can be generated using biomass fuelled boiler and injected to the air stream after the compressor. This will increase the total mass flow rate through the turbine without any additional load on the compressor, thus, increasing the net turbine output power without the need for excessive elevation in TIT. The performance of HAT cycle has been investigated in literatures [20]. However, to the authors knowledge, experimental testing of biomass fuelled HAT system based on turbocharger-EFGT cycle has not been reported in the literatures.

The current study aims at designing a small-scale biomass fuelled HAT system based on the existing EFGT test rig to determine the target boiler capacity for the system. After that, several steam generator configurations will be compared to choose the optimum design suitable for the HAT cycle. The complicated tube bank, inlet and outlet distributers and hundreds of welding points in the conventional boiler designs are entirely avoided in a mono-tube boiler design which adds the needed reliability for operating in rural areas with the absence of trained boiler operators. The optimum boiler design will be tested experimentally with biomass to characterize the performance of the boiler at wide range of steam flow rates before it can be tested with the HAT cycle in future work.

2. Materials and Methods

2.1 HAT System Design

Biomass fuelled EFGT system was developed and tested experimentally in previous study by Al-Attab and Zainal [21]. The system consisted of a dual chamber gasifier-combustor, two-pass shell-and-tube stainless steel (SS) heat exchanger, Holset H1C truck turbocharger and turbocharger cooling/lubrication unit [21]. Several turbine start-up methods were tested, but the turbine was not able to operate in self-sustaining mood due to the low TIT [17]. In the current study, a new HAT system was designed based on the accumulated experience from the previous EFGT system. The new system design includes a more efficient Garrett GT25 turbocharger with ball-bearings since it can provide significantly lower turbine start-up requirement. The efficiency of this turbocharger was shown in literatures [13], enabling it to sustain stable operation at a significantly lower pressure of 0.1 bar compared to 0.4 bar for the Holset H1C. From the compressor and turbine performance maps for Garrett GT25, turbine and compressor efficiencies are 70% and 65%, respectively, at air flow rate of 0.11 kg/s and pressure ratio of 2.

Using off-cut furniture wood, the combustor temperature was limited in the range of 900-1100°C when using cold air supply for the gasifier-combustor. However, full recuperation of the hot air after the turbine back to the chamber elevated chamber temperature exceeding 1300°C. For the new HAT cycle design, 50% of the hot air will be recuperated to the gasifier combustor to maintain chamber temperature at 1200°C. However, since steam is injected into the air stream after the combustor, the effect of steam on the performance of the gasifier-combustor has to be considered. On one hand, the quality of the gas product from the gasifier can be improved through the steam-air gasification. On the other hand, steam flow rate has to be within the acceptable steam-to-biomass ratio (S/B) to avoid temperature drop in the gasifier due to the excessive amount of steam. Maximum S/B ratio in the literature was found to be in the range of 1.2-2.5 [22,23]. Therefore, maximum steam flow rate of 2 kg/min was chosen in this design, which corresponds to about 2.4 S/B ratio at 50% hot air recuperation. Detailed energy balance of the calculated HAT system design is shown in Figure 1. Thermal output of the HAT system is 40.7 kW with overall system efficiency of 37.8%.

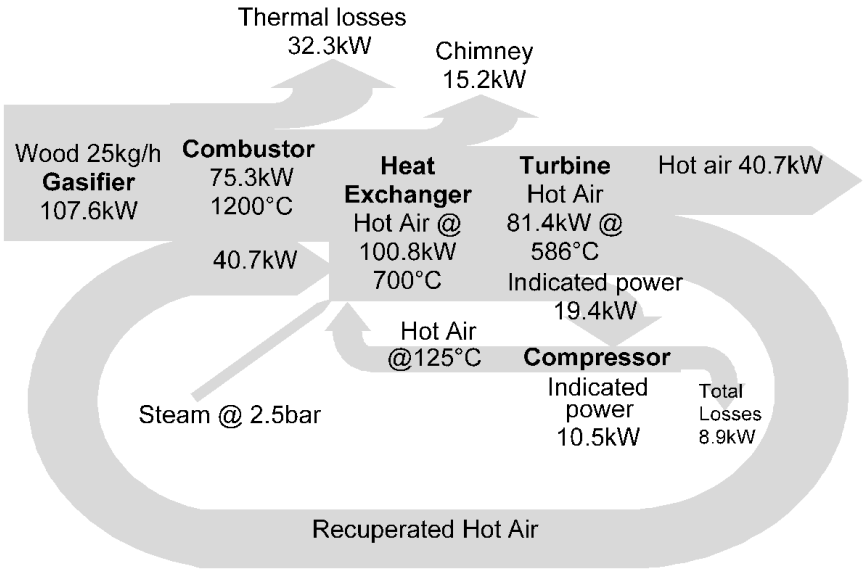

Fig. 1. Sankey-diagram of the energy flow of the new HAT system

2.2 Boiler Design

In order to convert the EFGT cycle into HAT cycle, steam will be injected into the compressed air stream after the compressor. The boiler will utilize same waste biomass off-cut furniture wood used in the gasifier-combustor. The design is based on the ASME Standard: PTC-4-1 Power Test Code for Steam Generating Units. Mono-tube coil configuration was chosen to avoid any welding joint in the boiler design. This will increase the reliability of the boiler to be suitable for the operation in rural places with low maintenance requirement, as well as simplifying the fabrication process since the need for tube cutting and welding are eliminated.

A mathematical model was developed for the optimization of the boiler geometry and operating conditions. Two tube configurations were considered for the design to achieve the target steam flow rate of 2 kg/min: the counter flow and parallel flow. Also, two steam output temperatures of 135°C and 145°C were evaluated in the design and both temperatures exceeded the target compressor output pressure of 2 bar. Three cupper coil tube sizes of 6, 8 and 10mm inner diameter (Di) were compared for both parallel and cross flow configurations. Copper was chosen as the preferable material for the coil due to its higher thermal conductivity. The mathematical model will provide the required tube coil length (L) to achieve the target steam temperature and flow rate for the different designs, and the boiler will be fabricated based on the optimum (L) value. The coil length calculations for each configuration were divided into two sections: water preheater and evaporator. Water is heated inside the preheater tube in an isobaric sensible heating manner where water temperature increases from 30°C up to the design boiling temperature (i.e. 135°C or 145°C). Once water reaches the boiling temperature, it starts to evaporate in an isothermal-isobaric manner and the latent heat of evaporation is taken from the steam properties table. For the parallel flow configuration, the bottom part of the coil at the hot zone above the furnace is filled with liquid water presenting the preheater above the furnace compared to saturated steam for the counter flow as shown in Figure 2. With the target boiler efficiency of 70%, wood consumption is calculated first. The calculated stoichiometric air/fuel ratio for wood ($CH_{1.4}O_{0.71}N_{0.01}$) is 5.5. Therefore, the required air flow is 0.053kg/s (assuming 20% excess air) and the flue gas flow rate is 0.061kg/s.

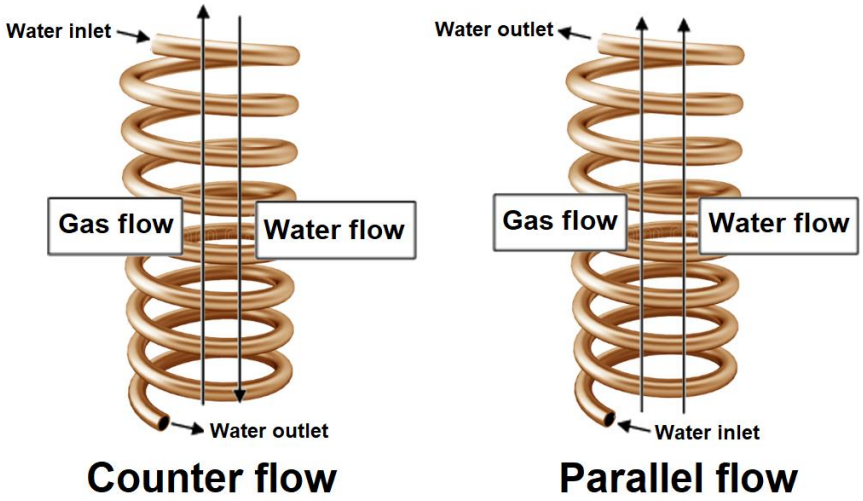

Fig. 2. Counter and parallel flow configurations for the mono-tube boiler

Despite having similar heat transfer setup between the hot gas and the tube where the gas passes across the tubes in cross flow manner, the significant difference in heat transfer performance between the two configurations is due to the difference in temperature levels between inner and outer fluids. The heat transfer from the hot gas to water is calculated based on the convection heat transfer as well as the radiation from the flame. For the convection heat transfer, $T_{gas\text{-}in}$ =900°C was considered for the average flue gas temperature while higher value of T_f =1000°C was estimated for the average flame temperature for wood combustion for the radiation heat transfer calculations. The Log-Mean Temperature Difference design method was used for the estimation of the required heat transfer surface area based on the heat balance of the heat exchanger. The heat required for water boiling (Q_{water}) is equal to the heat supplied from the combustion through convection (Q_c) and radiation (Q_r) as shown in Eq. (1) [24].

$$Q_{water} = Q_c + Q_r = UA\Delta T_{lm} \tag{1}$$

The required length of the coil is calculated using Eq. (2).

$$L = \frac{A_c}{\pi Do} \tag{2}$$

where (U) is the overall heat transfer coefficient, (A_c) is the coil convection heat transfer area and (Do) is the outer pipe dimeter of the mono-tube coil. Radiation heat supply is calculated using Eq. (3) [25].

$$Q_r/A_r = \varepsilon\sigma T_f^4 \tag{3}$$

where (σ) is the Stefan–Boltzmann constant and (ε) is the flame emissivity which is calculated using Eq. (4) [25].

$$\varepsilon = 1 - e^{(-kl)} \tag{4}$$

where (k) is the effective emission coefficient (m^{-1}) which is about 0.8 for wood combustion, and (l) is the mean equivalent beam length of the flame (m), which is approximated as the flame radius from the chamber geometry. Standard metal barrel of 200L capacity was chosen as the outer shell of the

boiler and the furnace beneath the drum has similar diameter of 0.6m. Radiation surface area (A_r) was approximated to a cylindrical surface area presenting the coil winding height and diameter facing the radiation from the flame. Therefore, (A_r) can be calculated directly from (L).

Figure 3 shows the flowchart of the mathematical model for boiler design. Initially, the input data to the model is divided into two categories: geometry parameters and operating parameters. Geometry parameters include the tube diameter, shell diameter and (L) while the operating parameters include the inlet and outlet temperatures and flow rate for steam and flue gas. The overall heat transfer coefficient is calculated first in order to determine the required heat transfer surface area. From the surface area, the length of the tube (L) is calculated and the value is inserted back to the geometry parameters. The iterations continue until the difference between the calculated (L) value in two subsequent iterations drop below 0.1 m, then the calculation is considered converged. The radiation surface area (A_r) can be calculated after that from (L) in each iteration, which allows the recalculation of the temperature balance. However, since steam inlet and outlet temperatures are fixed, as well as the flue gas inlet temperature, the only value that can be manipulated is flue gas exit temperature ($T_{gas\text{-}out}$). Therefore, this new value is inserted back to the operating parameters. The iterations continue until the difference between the calculated ($T_{gas\text{-}out}$) value in two subsequent iterations drop below 1°C, then the calculation is considered converged.

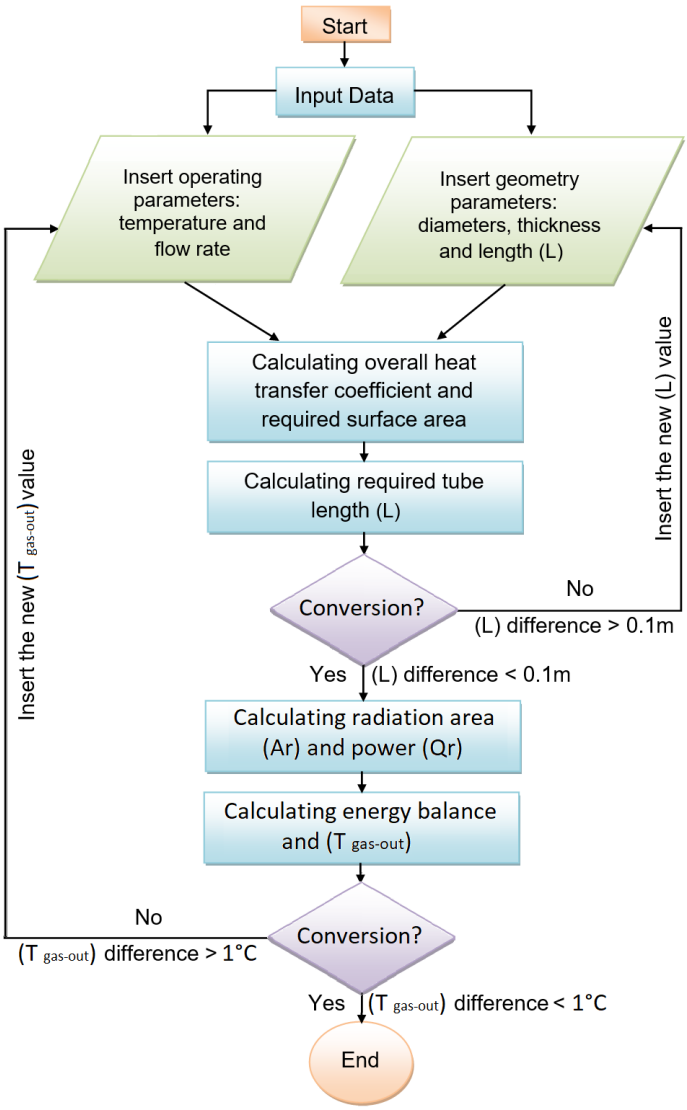

Fig. 3. Flowchart of the boiler design mathematical model

2.3 Experimental Setup and Measurement

The system experimental test rig and auxiliary equipment consist of the boiler, water pump, air blower, temperature data logger and mass balance as shown in Figure 4. Biomass fuel used for the experiment is off-cut furniture wood waste. The mass of the fuel is determined before feeding into the biomass furnace for the periodic measurement of the fuel consumption. The air flow rate through the boiler is measured using hot-wire anemometer at the blower inlet and the intensity of the flame inside the furnace is controlled by the air flow supply. Blower rotating speed was controlled via a frequency invertor. The water supply system is shown in Figure 5. From the figure, the main outlet (1) from the water pump was directly supplied into the coil inside the boiler, while the main inlet (5) was connected to the existing water tank which store the water supply for the whole system. The bypass outlets (3) and (4) allow the excessive water to flow back into the tank. The safety outlet (2) opens automatically whenever the system encounters high pressure due to back-pressure flow exceeding 3 bar. Water supply flow to the water pump is measured by a graduated tube for water volume measurement and a stopwatch. Water/steam pressure was measured using 10 bar pressure gauge on the water pump. Temperature was measured at the boiler outlet using type-K thermocouple and the temperature profile was recorded in a 12-channel data-logger.

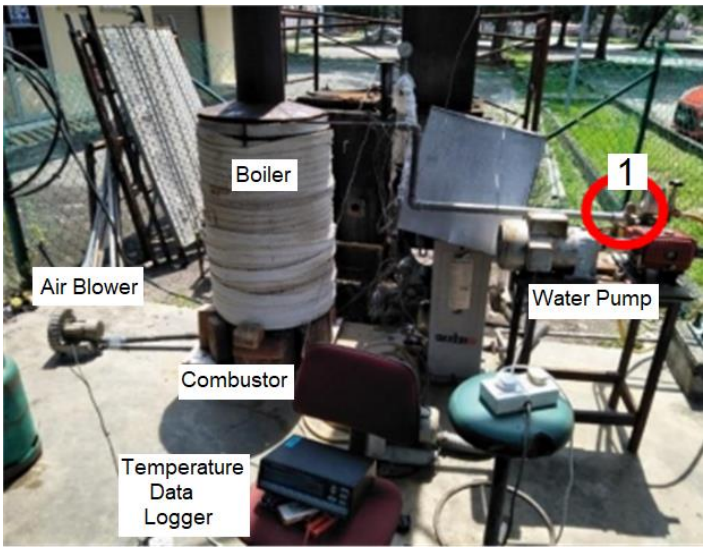

Fig. 4. Experimental set-up for the mono-tube boiler

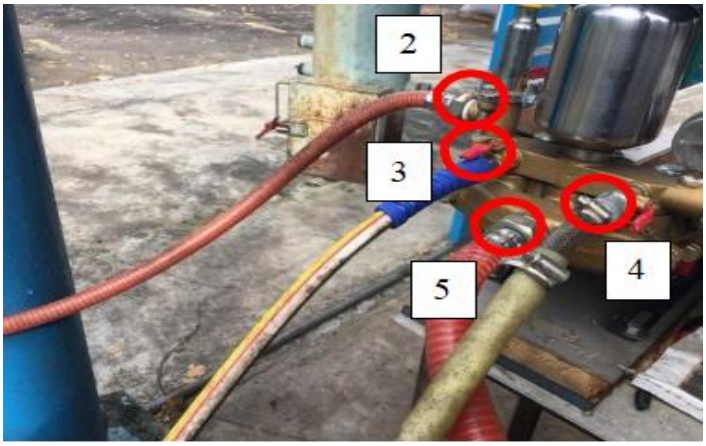

Fig. 5. Water supply system and water pump

2.4 Performance Characterization

The optimum boiler design was characterized experimentally at a wide range of steam flow rates. Several biomass feeding cycles are performed, and average biomass fuel consumption is calculated. Biomass thermal input power to the boiler is calculated using Eq. (5).

$$Q_{biomass}(kW) = \left[\dot{m}\left(\frac{kg}{s}\right) \times LHV\left(\frac{kJ}{kg}\right)\right]_{biomass} \quad (5)$$

where the average lower heating value (LHV) of the off-cut furniture wood used in the experiment was about 15.4 MJ/kg with average moisture content of 11%. The output power of the boiler is the steam thermal power that can be calculated from the change in enthalpy from 30°C up to the outlet steam temperature using Eq. (6).

$$Q_{steam}(kW) = \left[\dot{m}\left(\frac{kg}{s}\right) \times \Delta h\left(\frac{kJ}{kg}\right)\right]_{steam} \quad (6)$$

Thermal efficiency of the boiler as the main performance indicator can be then calculated using Eq. (7).

$$\eta_{boiler} = [Q_{steam}/Q_{biomass}] \times 100 \quad (7)$$

Another factor that indicates the performance of the boiler in terms of its fuel economy is the specific fuel consumption (SFC) calculated using Eq. (8).

$$SFC(kg_{fuel}/kW.h) = \frac{\text{Fuel consumption rate } (kg/h)}{Q_{steam}\ (\text{kW})} \quad (8)$$

3. Results and Discussions

3.1 Effect of Flow Configuration on Boiler Design

The evaluation included the suitable steam output temperature where two values of 135°C and 145°C were compared. For the comparison, three copper tube inner diameters of 10, 8 and 6 mm were chosen. The required energy to elevate water temperature from 30 to 135°C was 14.7kW compared to 16kW at the higher temperature, unlike the case for the evaporator which has the reverse effect. The higher steam temperature target requires less specific energy of 2129 kJ/kg for the evaporation compared to 2159 kJ/kg for the lower temperature. The latent heat required for the evaporation presented nearly five folds of the sensible heat in the pre-heater. Therefore, having lower latent heat of evaporation at 145°C resulted in a considerably lower overall tube length (L) of about 15% for counter flow and 13% for parallel flow. The other investigated factor is the inner tube diameter. In general, the effect of the tube diameter on the overall tube length is controversial. On one hand, reducing the diameter helps in the reduction in (L) through the enhancement in heat transfer inside the tube by elevating Reynolds number. On the other hand, for the same heat transfer area, smaller diameter with results in higher (L) value through the geometry calculations. This resulted in about 26% reduction in overall (L) when (D_i) was increased from 6mm to 10mm for counter flow and 27% for parallel flow. Tube length (L) and surface area (A_c) is summarized for all the investigated configurations in Table 1.

Table 1
Estimated copper length in meters

Configuration type	Counter Flow						Parallel Flow					
	Steam outlet temperature (°C)											
	135			145			135			145		
	Tube inner diameter (mm)											
	6	8	10	6	8	10	6	8	10	6	8	10
Preheater (A_c), m^2	0.33	0.39	0.46	0.37	0.43	0.52	0.14	0.16	0.20	0.16	0.18	0.23
Preheater (L), m	17.7	15.5	14.9	19.6	17.2	16.5	7.6	6.7	6.4	8.6	7.5	7.2
Evaporator (A_c), m^2	2.82	3.08	3.39	2.32	2.52	2.78	3.2	3.5	3.9	2.8	3.1	3.4
Evaporator (L), m	150	123	108	123	101	88.5	175	143	126	151	123	109
Total (A_c), m^2	3.16	3.47	3.86	2.68	2.96	3.30	3.3	3.6	4.16	2.99	3.3	3.6
Total (L), m	167.7	138.2	122.9	142.5	117.7	105	182.8	150	132.5	159.2	130.7	115.6

The major factor in boiler design is the flow configuration, and a comparison between the counter flow and parallel flow is illustrated in Figure 6. The results indicated that counter flow configuration provided better overall heat transfer performance compared to the parallel flow. The required total length of copper for parallel flow was higher than counter flow by 8-10% through all the different configurations. Optimum boiler design included 10mm tube diameter, 145°C steam temperature and counter flow configuration with total tube length of 105m.

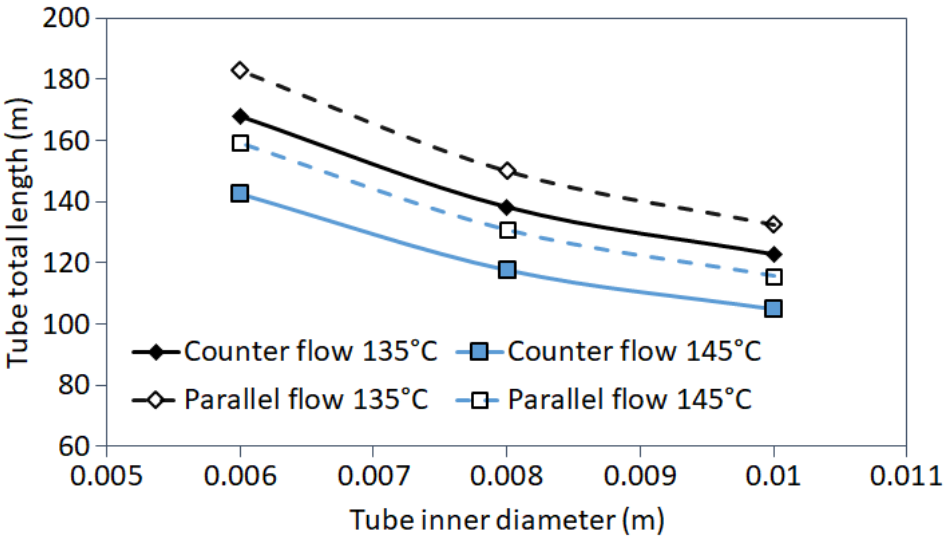

Fig. 6. Calculated total tube length at different stem temperatures and tube inner diameters

Temperature profile comparison between counter and parallel flow configurations for 10mm tube diameter is illustrated in Figure 7. The boiler tube side (dash-lines) contains two zones: preheater and evaporator. The preheater elevates water temperature up to the design boiling temperature (i.e. 135°C or 145°C) in a sensible heating manner. Once water reaches the boiling temperature, evaporation starts in a latent heat manner at constant temperature and pressure. Gas inlet temperature is fixed at 900°C for both configurations, but the drop in temperature varied considerably showing high drop of 12°C/m for parallel flow compared to 5°C/m for counter flow. This can be explained by the higher heat transfer for the water-to-gas flow in the preheater compared to gas-to-gas flow in the evaporator. However, the parallel flow configuration suffered from lower gas

temperature drop of 2.8°C/m through the evaporator since gas enters the evaporator zone at lower temperature of 721°C compared to 900°C for the counter flow. Overall average temperature drop for the counter flow was 5.2°C/m compared to 4°C/m for the parallel flow. This resulted in about 10 m difference in the required tube length for the heat transfer, and about 80°C difference in chimney temperature.

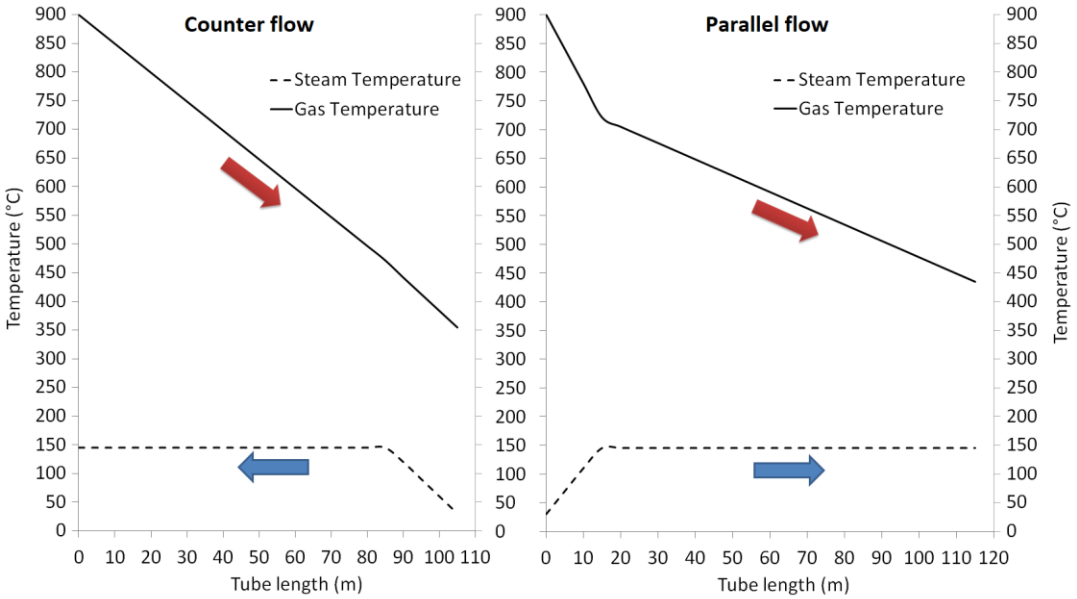

Fig. 7. Sample of the temperature profiles for the design of the different sections of the boiler

3.2 Experimental Performance of the Boiler

The boiler was characterized in wide range of steam flow rates in the range of 0.47-2 kg/min. Steam was discharged directly to the ambient at the boiler exit, thus, boiler pressure was limited to slightly above atmospheric pressure. When the steam feeding is connected to the compressor outlet, the back-pressure will elevate the steam pressure automatically and the piston pump is capable of providing the needed pressure to overcome the pressure drop in the coil and the back-pressure from the compressed air. Input thermal power from biomass depends on the rate of wood consumption and it was elevated from 29kW up to 103 kW. The respond from steam was linearly proportional to the power input in the range of 18-75 kW as shown in Figure 8.

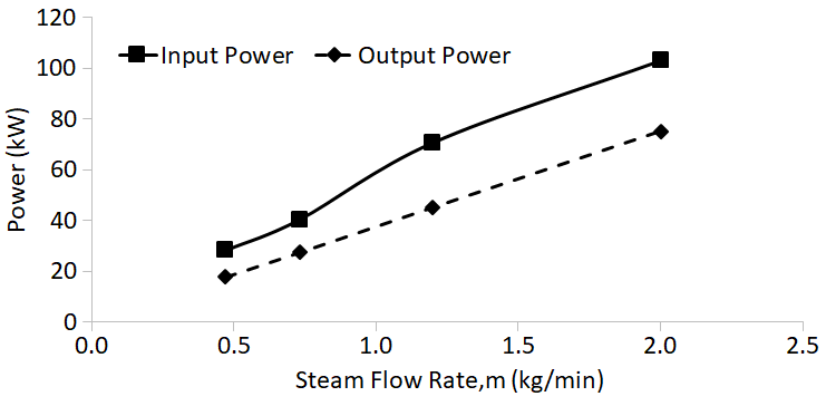

Fig. 8. Biomass input power and steam output power at different steam flow rates

The feeding rate of biomass was controlled to maintain steam temperature in the range of 110-120°C. Thus, lower steam flow inside the tube was associated with lower flue gas flow rate, which reduced the heat transfer and affected thermal efficiency of the boiler negatively. Minimum boiler efficiency was 61% at the lowest steam flow rate while maximum efficiency was 73% at the target steam flow of 2 kg/min. The efficiency was not linear as the thermal power of steam as can be seen in Figure 9. This can be explained by the fluctuation in heat transfer quality as the heat input fluctuate with the inconsistent biomass combustion. The specific fuel consumption (SFC) is another important factor that indicates the fuel economy. The SFC is directly related to the efficiency but in reversed proportional pattern. The lowest efficiency resulted in higher fuel consumption of 0.35kg/kWh which reduced down to 0.29 at maximum efficiency.

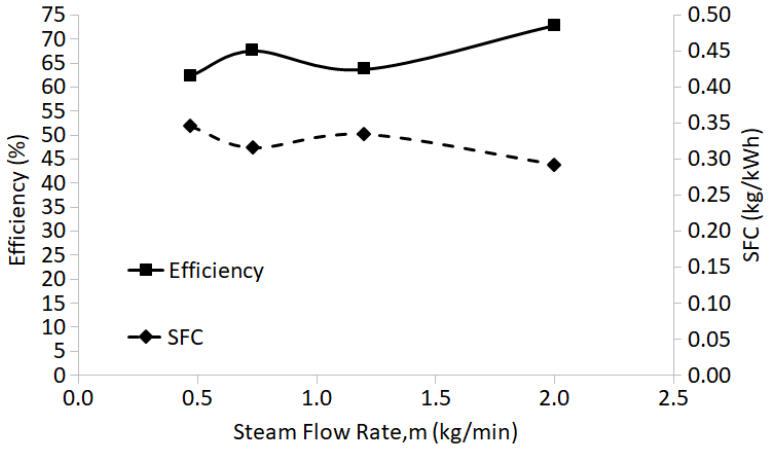

Fig. 9. Boiler efficiency (%) Vs Water Flow Rate (kg/min)

The fluctuation in combustion showed a direct effect on the steam output temperature as illustrated in the time profile for steam temperature for the different flow rates in Figure 10. The fluctuation is minimal at low flow rates since the amount of biomass contained in the furnace is limited with low flame height. However, when biomass feeding is increased, the height of the wood stock increases irregularly as wood blocks are pushed to the chamber. Therefore, flame fluctuation leads to irregular movement of the flame tips that come close or touch the coil bottom resulting in sudden spikes in steam temperature especially at the highest combustion intensity and steam flow of 2 kg/min.

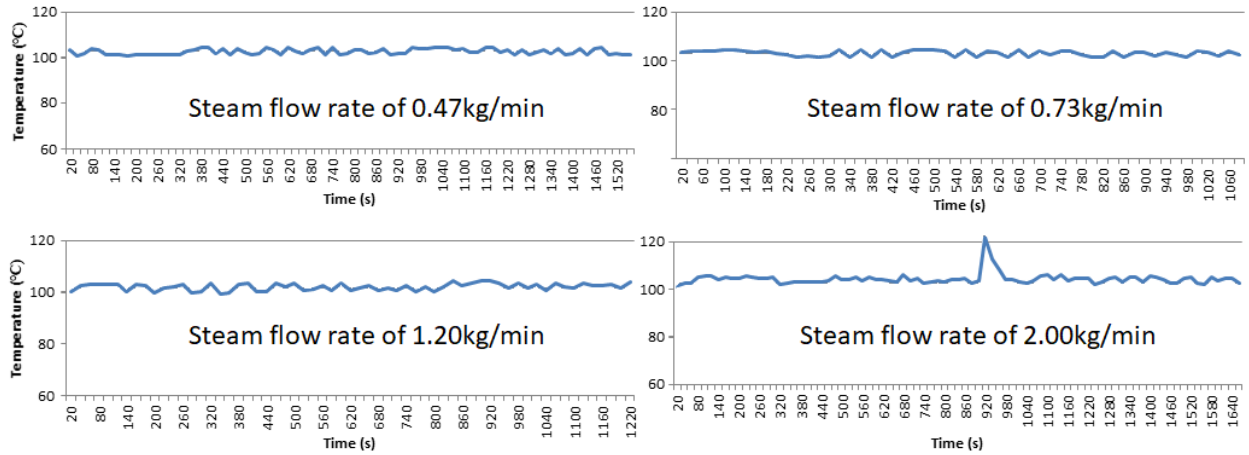

Fig. 10. Steam Temperature profiles at steady-state operation for the different flow rates

4. Conclusions

The design and energy balance of the HAT cycle was achieved based on the experience gained from the previously tested externally gas turbine system. Mathematical model was developed to optimize the mono-tube boiler design for the HAT cycle. Two configurations of counter and parallel flow arrangement were compared with different tube diameters and steam target temperatures. Minimum copper tube length of 105 meter was achieved using counter flow configuration with 10mm tube diameter and target steam temperature of 145°C and boiler efficiency of 70%. The boiler was developed and tested experimentally with biomass off-cut furniture wood. Stable boiler operation and steam production was achieved for the full steam flow rate range of 05-2 kg/min. The increase in steam and flue gas flow rate enhanced considerably the heat transfer and boiler thermal efficiency from 61% up to 73%. Fuel economy was also improved as indicated by the drop in fuel consumption from 0.35 kg/kWh down to 0.29 kg/kWh.

Acknowledgement

The authors would like to thank the Ministry of Education Malaysia, Fundamental Research Grant Scheme (FRGS) No.: 203.PMEKANIK.6071426 for the financial support of this study.

Reference

[1] Sorrentino, Arianna, Antonio M. Pantaleo, Niccolò Le Brun, Salvador Acha, Christos N. Markides, Giacobbe Braccio, Emanuele Fanelli, and Sergio M. Camporeale. "Energy performance and profitability of biomass boilers in the commercial sector: A case study in the UK." *Energy Procedia* 148 (2018): 639-646. https://doi.org/10.1016/j.egypro.2018.08.152

[2] Shafiee, Shahriar, and Erkan Topal. "When will fossil fuel reserves be diminished?." *Energy Policy* 37, no. 1 (2009): 181-189. https://doi.org/10.1016/j.enpol.2008.08.016

[3] Coady, David, Ian Parry, Nghia-Piotr Le, and Baoping Shang. "Global fossil fuel subsidies remain large: an update based on country-level estimates." *International Monetary Fund (IMF) Working Papers* 19, no. 89 (2019): 39. https://doi.org/10.5089/9781484393178.001

[4] Wang, Zhaohua. "Does biomass energy consumption help to control environmental pollution? Evidence from BRICS countries." *Science of the Total Environment* 670 (2019): 1075-1083. https://doi.org/10.1016/j.scitotenv.2019.03.268

[5] Burke, Matthew J., and Jennie C. Stephens. "Political power and renewable energy futures: A critical review." *Energy Research & Social Science* 35 (2018): 78-93. https://doi.org/10.1016/j.erss.2017.10.018

[6] Din, Zia Ud, and Z. A. Zainal. "Biomass integrated gasification-SOFC systems: Technology overview." *Renewable and Sustainable Energy Reviews* 53 (2016): 1356-1376. https://doi.org/10.1016/j.rser.2015.09.013

[7] Zakaria, A., Firas B. Ismail, MS Hossain Lipu, and M. A. Hannan. "Uncertainty models for stochastic optimization in renewable energy applications." *Renewable Energy* 145 (2020): 1543-1571. https://doi.org/10.1016/j.renene.2019.07.081

[8] Panwar, N. L., S. C. Kaushik, and Surendra Kothari. "Role of renewable energy sources in environmental protection: A review." *Renewable and Sustainable Energy Reviews* 15, no. 3 (2011): 1513-1524. https://doi.org/10.1016/j.rser.2010.11.037

[9] Kozlov, Alexander, Oleg Marchenko, and Sergei Solomin. "The modern state of wood biomass gasification technologies and their economic efficiency." *Energy Procedia* 158 (2019): 1004-1008. https://doi.org/10.1016/j.egypro.2019.01.244

[10] Nakahara, Yuka, Tomohiro Tabata, Tomoko Ohno, Fumiko Furukawa, Katsuro Inokuchi, Keiko Katagiri, and Yosuke Hirayama. "Discussion on regional revitalization using woody biomass resources as renewable energy." *International Journal of Energy and Environmental Engineering* 10, no. 2 (2019): 243-256. https://doi.org/10.1007/s40095-019-0300-5

[11] Anuar, M. S., Khaled A. Al-attab, and Z. A. Zainal. "Gasifier-torrefier using syngas as the thermal agent." *Energy Conversion and Management* 149 (2017): 79-86.

https://doi.org/10.1016/j.enconman.2017.06.085
[12] Patuzzi, Francesco, Dario Prando, Stergios Vakalis, Andrea Maria Rizzo, David Chiaramonti, Werner Tirler, Tanja Mimmo, Andrea Gasparella, and Marco Baratieri. "Small-scale biomass gasification CHP systems: Comparative performance assessment and monitoring experiences in South Tyrol (Italy)." *Energy* 112 (2016): 285-293. https://doi.org/10.1016/j.energy.2016.06.077
[13] Enagi, Ibrahim I., Khaled A. Al-Attab, and Z. A. Zainal. "Combustion chamber design and performance for micro gas turbine application." *Fuel Processing Technology* 166 (2017): 258-268. https://doi.org/10.1016/j.fuproc.2017.05.037
[14] Khattak, M. A., N. S. Mohd Ali, N. H. Zainal Abidin, N. S. Azhar, and M. H. Omar. "Common Type of Turbines in Power Plant: A Review." *Journal of Advanced Research in Applied Sciences and Engineering Technology* 3, no. 1 (2016): 77-100.
[15] Orozco, Dimas José Rúa, Osvaldo José Venturini, and José Carlos Escobar Palácio. "Parametric analysis of an externally fired-gas turbine (EFGT): effect of main parameters over the power generated, cycle efficiency and exergy destruction." In *23rd ABCM International Congress of Mechanical Engineering. Anais*. 2015. https://doi.org/10.20906/CPS/COB-2015-0847
[16] Baten, Tasmia, Dara Abdus Satter, Rezwanul Ahsan, and Ashraful Hoque. "Simple Modelling and Analysis of Operating Parameter of Externally Fired Micro Gas Turbine Using Biomass." In *2018 7th International Conference on Computer and Communication Engineering (ICCCE)*, pp. 1-6. IEEE, 2018. https://doi.org/10.1109/ICCCE.2018.8539275
[17] Al-attab, Khaled A., and Z. A. Zainal. "Turbine startup methods for externally fired micro gas turbine (EFMGT) system using biomass fuels." *Applied Energy* 87, no. 4 (2010): 1336-1341. https://doi.org/10.1016/j.apenergy.2009.08.022
[18] Durão, Luís, Margarida Gonçalves, Catarina Nobre, Octávio Alves, Paulo Brito, and Benilde Mendes. "Production of High Calorific Value Biochars by Low Temperature Pyrolysis of Lipid Wastes and Lignocellulosic Biomass." In *International Conference on Innovation, Engineering and Entrepreneurship*, pp. 655-661. Springer, Cham, 2018.
[19] Al-Attab, Khaled A., and Z. A. Zainal. "Externally fired gas turbine technology: A review." *Applied Energy* 138 (2015): 474-487. https://doi.org/10.1016/j.apenergy.2014.10.049
[20] Nyberg, Björn, and Marcus Thern. "Thermodynamic studies of a HAT cycle and its components." *Applied Energy* 89, no. 1 (2012): 315-321. https://doi.org/10.1016/j.apenergy.2011.07.036
[21] Al-Attab, Khaled A., and Z. A. Zainal. "Performance of high-temperature heat exchangers in biomass fuel powered externally fired gas turbine systems." *Renewable Energy* 35, no. 5 (2010): 913-920. https://doi.org/10.1016/j.renene.2009.11.038
[22] Sharma, Shweta, and Pratik N. Sheth. "Air-steam biomass gasification: experiments, modeling and simulation." *Energy Conversion and Management* 110 (2016): 307-318. https://doi.org/10.1016/j.enconman.2015.12.030
[23] Andrew, Renny, D. T. Gokak, Pankaj Sharma, and Shalini Gupta. "Practical achievements on biomass steam gasification in a rotary tubular coiled-downdraft reactor." *Waste Management & Research* 34, no. 12 (2016): 1268-1274. https://doi.org/10.1177/0734242X16659352
[24] Shah, Ramesh K., and Dusan P. Sekulic. *Fundamentals of Heat Exchanger Design*. John Wiley & Sons, 2003. https://doi.org/10.1002/9780470172605
[25] Drysdale, Dougal. *An Introduction to Fire Dynamics*. John Wiley & Sons, 2011. https://doi.org/10.1002/9781119975465